Original Research Article

Screening of high-NMN-producing natural strains and biosynthesis of NMN using Nampt

Chao Li[1,2,3,#], Zouguo Long[1,#], Haichao Zhang[1,#], Yuhui Lin[4], Liqing Zhao[1,*]

[1] *Department of Food Science and Technology, College of Chemistry and Environmental Engineering, Shenzhen University, Shenzhen 518060, Guangdong Province, China*

[2] *College of Physics and Optoelectronic Engineering, Shenzhen University, Shenzhen 518060, Guangdong Province, China*

[3] *Hanshan Normal University, Chaozhou 521000, Guangdong Province, China*

[4] *Shantou Tianyue Technology Innovation Research Institute Co., Ltd., Shantou 515063, Guangdong Province, China*

* Corresponding author: Liqing Zhao, lqzhao@szu.edu.cn

# These authors contributed equally to this work.

Abstract: Nicotinamide mononucleotide (NMN) is an endogenous substance in humans with high safety and thermal stability, and its application in cosmetics, medical health, and functional foods has received widespread attention. However, the synthesis process of NMN has problems, such as high cost, time-consuming process, and low yield, which limits the large-scale industrial application of NMN to a certain extent. Nicotinamide phosphoribosyl transferase (Nampt) is a critical enzyme in the technical route of the biological synthesis of NMN, which can catalyze the synthesis of NMN using nicotinamide and phosphoribosyl pyrophosphate. The screening and expression of Nampt with excellent enzymatic properties and stability is the key to the synthesis of NMN via this method. At present, the main problems in the technical route of NMN production using Nampt are that the catalytic activity of Nampt is low and the sources of Nampt are limited. In this study, we isolated *Enterobacter chengduensis* 2021T4.7, a microorganism with a high NMN production, and optimized its fermentation condition. The yield of NMN was up to 67.66 μM. In addition, we synthesized Nampt and constructed related recombinant high-yield engineered bacteria. We semi-rationally designed a Nampt structure derived from mice and obtained mutant mNampt-V365L with NMN yield as high as 135.99 μM, which increased by 62% from that of the wild type. Here, we screened high-NMN-yield natural strains and obtained high-NMN-yield strains through the semi-rational design optimization of Nampt enzymes, which provided new chassis microorganisms and new ideas for the conversion rate of NMN.

Keywords: nicotinamide mononucleotide; fermentation conditions optimization; semi-rational design

1. Introduction

Nicotinamide mononucleotide (NMN), with the formula C11H15N2O8P, is associated with many diseases and has attracted much attention in recent years as a nutraceutical[1]. In the human body, NMN is converted to NAD^+, a coenzyme present in all living cells. The metabolism of NAD^+ is also associated with various physiological conditions and is essential in various metabolic reactions in the human body[2]. Studies have shown that NAD^+ muscle levels can be supplemented with NAD^+ precursors NMN and nicotinamide riboside (NR) in the diet[3]. Among the NAD^+ precursors, NMN is the best in improving intracellular NAD^+ in oral gavage mouse experiments. NMN is rapidly absorbed into NAD^+ in metabolic tissues within 30 min, and so it is suitable as NAD^+ supplementation[4,5]. In 2016, Uddin et al.[6] found that mice equivalent to 70 years old in human age returned to the 20-year-old state after taking NMN for one week, and the mice also lived 20% longer. In recent years, with the deepening of research on NMN, researchers have gradually realized the importance of the biological activity of NMN to life and health. NMN has particular applications in cosmetics, nutrition and health, functional food, and

other fields[7–9]. It has also been associated with aging-related degenerative diseases, neurodegenerative diseases, endocrine system balance, insulin secretion, diabetes, and obesity[10–15].

The biosynthetic NMN pathway includes the nicotinamide riboside (NR) phosphorylation pathway and the nicotinamide (NAM) salvage pathway (**Figure 1**). The production process of NMN by biosynthesis is simple, and the production process is environmentally friendly and pollution-free. The cost of NMN is high, and most of NMN raw materials are prepared via chemical synthesis. In addition, the organic solvents used in the production process are toxic, and the NMN produced often has problems, such as organic solvent residue, chirality, etc. In 2018, Marinescu et al.[16] invented a method for preparing NMN by microbial fermentation, where nicotinamide phosphate ribose transferase (Nampt) recombinant *Escherichia coli* (*E. coli*)-engineered bacteria was constructed and substrates nicotinamide (NAM) and lactose were added to ferment to produce NMN with a yield of 15.4 mg/L. The target product NMN was separated via molecular sieve chromatography, and the chromatogram analysis showed that many NAM substrates did not completely react to produce NMN[17]. High-density fermentation of engineered bacteria can be considered to improve NMN conversion.
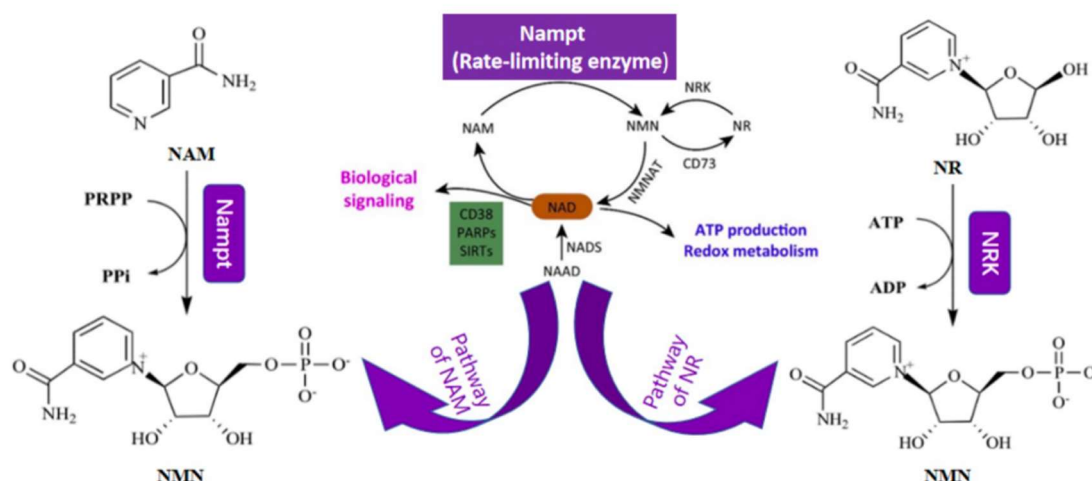
Figure 1. Biosynthetic pathway of NMN and salvage pathway of NMN in mammals.

Nampt is an important molecule in an organism's various life activities and energy metabolism, and mice that knock out this gene did not survive in experiments[13,18,19]. Nampt is an essential enzyme in the biosynthesis of NMN, catalyzing the synthesis of NMN using NAM and phosphoribosyl pyrophosphate (PRPP). Currently, there are few reports about Nampt's origins. Studies have shown that under the weak coupling of ATP hydrolysis and NMN synthesis, the catalytic efficiency of the human Nampt synthesis NMN system can be increased by 1100 times and the affinity for the NAM substrate is also greatly improved[20]. In recent years, there have also been research reports on applying Nampt expression in NMN production. Marinescu et al.[16] overexpressed Nampt derived from *Mus musculus*, *Shewanella oneidensis*, and *Haemophilus ducreyi* in *E. coli*, and NMN was produced by the addition of the NAM substrate during fermentation. Among them, the yield of NMN from *Haemophilus ducreyi*-derived Nampt expressed by *E. coli* reached 14.33 mg/L.

The screening and expression of Nampt with excellent enzymatic properties and stability have become the key to NMN biosynthesis. Directed protein evolution techniques have played an important role in synthetic biology and metabolic engineering and have been widely used to engineer enzyme molecules[21]. Enzymes can catalyze complex biochemical reactions in organisms under mild conditions. Most enzymes can be separated from organisms, but due to the influence of temperature, pressure, salt, and pH in the external environment, these natural enzymes in nature often fail to meet application needs in terms of enzyme activity, stability, specificity, and other aspects[22,23]. The directed evolution of proteins effectively solves the above problems[24].

The essence of the directed evolution of proteins[25] is to construct a library of protein molecular diversity and to screen out mutants with positive trait changes from the library. Semi-rational design is based on a series of algorithms and procedures developed in bioinformatics[26]. By simulating and designing to determine the mutation site of the gene of interest, the protein is optimized and modified in a targeted manner to build a high-quality screening library. Simply put, a semi-rational design is a random mutation in an artificially selected location or area. Many articles have reported using semi-rational design methods to improve the catalytic activity, stability, substrate specificity, etc., of enzymes[27–29].

In this study, high-NMN-yield natural strains were screened from soil, and their fermentation conditions were optimized. The semi-rational design optimization of the Nampt enzyme was carried out to significantly improve the conversion rate of NMN and provide new candidate strains and new Nampt enzyme sequences for low-cost production of NMN.

2. Screening and optimization of fermentation condition for high-NMN-yield strains

2.1. Screening of high-NMN-yield strains from soil

By enriching and screening microorganisms in the soil near the sewage outlet at Bangtai Bioengineering Co., Ltd., in Shenzhen, China, we isolated 396 strains. The strains were inoculated in a 96-well plate, where each strain carried out the enzyme conversion reaction at the same position as the enzyme plate. The amount of NMN produced was measured via the fluorescence method. The NMN content was determined based on the fluorescence values detected in each well, and strains with a stronger ability to convert nicotinamide into NMN were preliminarily screened out. We preliminarily selected 29 strains with high fluorescence values (above 4000) for further re-screening experiments (**Figure 2**). The 29 strains after initial screening were first inoculated in a nicotinamide-free Luria-Bertani (LB) medium. After the enzyme reaction system was determined (containing a buffer, a substrate, and a crude enzyme solution), seven high-NMN-yield strains were finally screened, of which strain 4-7 produced NMN with the highest concentration at 44.7 μM (**Figure 3**). Three strains with the highest NMN yield, which were strains 1-2, 3-4 and 4-7, were photographed under a microscope after Gram staining, where it was found that strain 1-2 was gram-positive, while strains 3-4 and 4-7 were gram-negative (**Figure 4**). The three strains were sent to Guangzhou Aiji Biotechnology Co., Ltd., for 16S rDNA sequencing identification. It was found that strain 1-2 belonged to the *Bacillus* genus, while strains 3-4 and 4-7 belonged to the genus Enterobacteriaceae. We named 4-7 as *Enterobacter chengduensis* 2021T4.7 and sent the strain to the China General Microbiological Culture Collection Center for preservation (culture preservation number: CGMCC No. 21695).

◇	1	2	3	4	5	6	7	8	9	10	11	12
A	3627	3829	3503	4560	2787	4927	2682	3928	2232	2544	2656	2586
B	4030	1850	2386	1499	1067	1203	1800	1304	1826	4667	1911	1799
C	4995	1866	1830	1007	2935	2643	1315	1917	2952	1599	1633	1884
D	1449	1219	2897	2829	1732	1821	2892	1628	2978	1165	1251	1267
E	1439	1939	1836	2957	2866	1012	2874	2806	1807	1386	1358	1370
F	1894	2870	1622	1009	2712	1638	1987	1976	1838	1136	1777	1838
G	1995	2609	1115	1619	1766	1551	1771	1865	1851	1846	1761	1761
H	1015	1759	1826	1917	1378	1761	4998	2583	1856	2981	1893	1872

◇	1	2	3	4	5	6	7	8	9	10	11	12
A	2420	1232	1635	2339	3939	4015	2572	4006	4667	1794	2205	3062
B	2140	2047	2130	1877	3908	1733	1653	2303	1824	1739	1801	1547
C	1639	1030	1904	1783	1575	1715	1658	3545	2501	1990	4974	1469
D	1733	1877	1992	1588	3084	1827	2579	1792	1750	5454	1622	1589
E	1686	1039	2001	1747	3244	2439	2386	1978	1718	1241	4711	1343
F	1605	1612	1783	1825	1315	1589	1699	4968	2383	1375	1394	1037
G	1355	1633	1939	2037	1438	1841	1942	1245	1147	1545	1951	1645
H	1825	1931	1735	3337	1638	1738	1839	1542	1448	1846	1751	2342

◇	1	2	3	4	5	6	7	8	9	10	11	12
A	4762	1432	3603	4619	4315	3045	2804	3289	3189	3257	2603	3331
B	4440	2194	3513	3713	3722	3483	2242	3188	2309	2448	2050	2405
C	3670	1891	2820	3059	2787	2904	2272	2541	2287	2383	2621	2430
D	3534	1960	2659	2710	2739	3164	1984	2314	2299	2472	2222	2141
E	3310	2619	3393	2823	2533	2480	1929	2237	2011	2081	2880	2219
F	4435	2198	2672	3040	2809	2525	1809	2381	2604	2657	2159	2276
G	3709	1966	2173	2896	3349	3109	2572	2756	2663	2919	2111	3331
H	3367	1909	3901	2658	2062	4405	2581	2625	4581	2471	2001	3999

◇	1	2	3	4	5	6	7	8	9	10	11	12
A	3784	3056	3097	2686	1972	4076	1882	2785	1997	3482	1237	3092
B	3381	3603	3230	5161	1971	2689	1385	1970	2265	2000	1454	1348
C	3617	5002	3125	2738	1200	3602	2051	2829	1312	3422	2263	1887
D	2543	2521	1863	3543	1914	2524	1958	3052	1898	1906	1926	1770
E	3061	5652	3371	2605	1721	3204	1695	2711	1627	5115	1377	2543
F	3317	2553	1915	2355	1792	2822	3151	3989	1719	4306	2449	2056
G	2448	2604	4456	2264	1000	5877	1691	2308	1955	3262	2246	4537
H	1551	1365	1210	1422	1245	1395	2247	2417	2332	3456	1372	1257

Figure 2. NMN content determination (fluorescence value data).
Note: Numbers marked in red are fluorescent values higher than 4000.
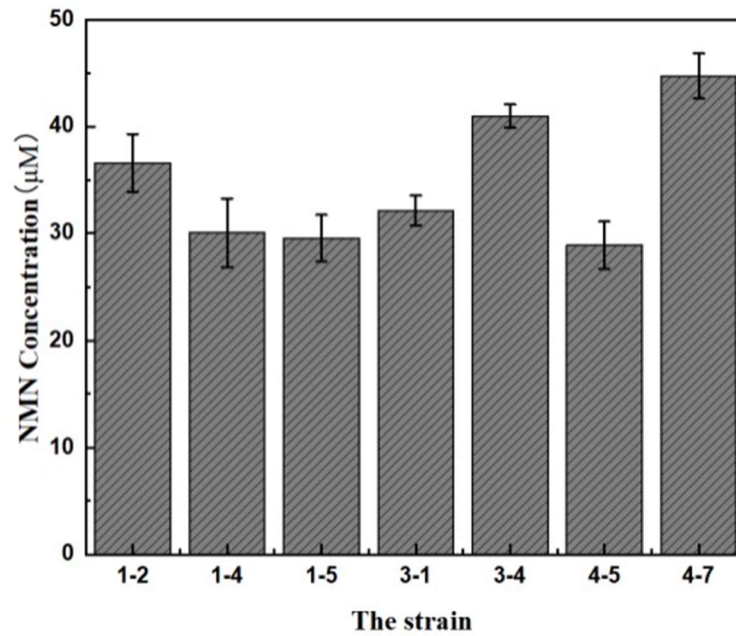
Figure 3. Yields of NMN produced by strains.

Figure 4. Gram staining results: strain 1-2 (left), strain 3-4 (middle), and strain 4-7 (right).

2.2. Fermentation medium optimization of strain *Enterobacter chengduensis* 2021T4.7

2.2.1. Carbon-source optimization of fermentation medium

First, we tested the effects of seven common carbon sources on the growth and NMN production of *Enterobacter chengduensis* 2021T4.7. Under the condition of uniformly adding a 1% carbon source, the growth of bacteria was judged by measuring the OD_{600} value, and the amount of NMN produced was measured using the fluorescence method. For the growth of *Enterobacter chengduensis* 2021T4.7 strain, the result showed that the best carbon source was rhamnose, followed by glucose, soluble starch, sucrose, and maltose. For the NMN production capacity of *Enterobacter chengduensis* 2021T4.7, the best carbon source was glucose, followed by soluble starch and rhamnose (**Figure 5(A)**). Considering that the primary purpose of this study was to improve the NMN-producing capacity of the *Enterobacter chengduensis* 2021T4.7 strain, we selected glucose as the carbon source for subsequent optimization. Subsequently, we used glucose as the carbon source to detect the effect of different glucose contents on NMN production. It can be seen that the higher the glucose content, the more favorable the growth of *Enterobacter chengduensis* 2021T4.7, but the change was minimal (**Figure 5(B)**). For the capacity of *Enterobacter chengduensis* 2021T4.7 to produce NMN, the NMN yield was

highest at 47.36 µM when 1% glucose was added. Therefore, 1% glucose was added to the fermentation medium as the carbon source in subsequent experiments.
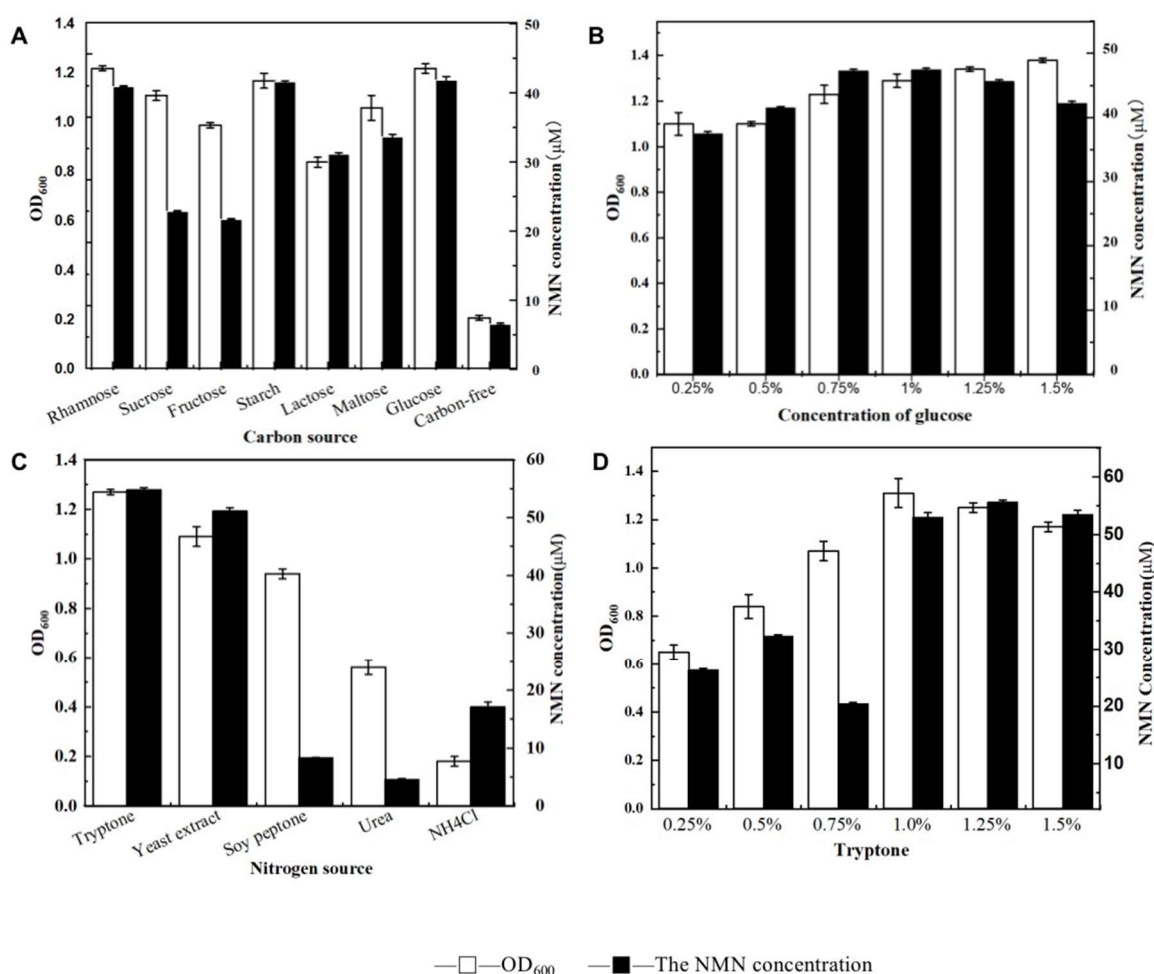
Figure 5. Effects of carbon and nitrogen sources on *Enterobacter chengduensis* 2021T4.7's cell growth and NMN production: **(A)** different carbon sources, **(B)** different glucose concentrations, **(C)** different nitrogen sources, and **(D)** different tryptone concentrations.

2.2.2. Nitrogen-source optimization of fermentation medium

Common sources of inorganic nitrogen include ammonium salts and nitrates, while common sources of organic nitrogen are mainly tryptone, soy peptone, and yeast extract. In this study, five common nitrogen sources were studied in a medium containing a 1% nitrogen source to explore the effects of nitrogen source types on the growth and NMN production of *Enterobacter chengduensis* 2021T4.7. It can be seen from **Figure 5(C)** that the best nitrogen source for the growth of *Enterobacter chengduensis* 2021T4.7 was trypsin, followed by yeast extract and soy peptone. For the capacity of *Enterobacter chengduensis* 2021T4.7 to produce NMN, the best nitrogen source was tryptone, with NMN yield of 54.83 µM, followed by yeast extract and NH$_4$Cl. Therefore, in the following studies, tryptone was chosen as the nitrogen source for the fermentation medium. We further studied the effects of different tryptone contents on the amount of NMN produced by *Enterobacter chengduensis* 2021T4.7. It can be seen from **Figure 5(D)** that the density of *Enterobacter chengduensis* 2021T4.7 first increased and then decreased with the increase in tryptone concentration. The addition of 1% tryptone was the most beneficial for growth. Similarly, for the capacity of *Enterobacter chengduensis* 2021T4.7 to produce NMN, the NMN yield was highest at 55.67 µM when 1.25% tryptone was added.

2.2.3. Mineral optimization of fermentation medium

Mineral elements are an essential part of the cell structure of microorganisms and are essential nutrients for microbial growth. Among them, phosphorus is one of the essential elements for microbial growth, which needs to be balanced with carbon and nitrogen. Excessive or insufficient phosphorus can affect the growth and energy synthesis of microorganisms, thereby affecting cell growth and metabolic activity. We investigated the effects of different levels of KH_2PO_4 on the growth of the *Enterobacter chengduensis* 2021T4.7 strain and its NMN-producing capacity. Adding 0.25% KH_2PO_4 was most beneficial for cell growth, but NMN yield was highest at 56.35 μM when 0.75% KH_2PO_4 was added (**Figure 6(A)**). Therefore, 0.75% KH_2PO_4 was added to the fermentation medium in subsequent experiments.
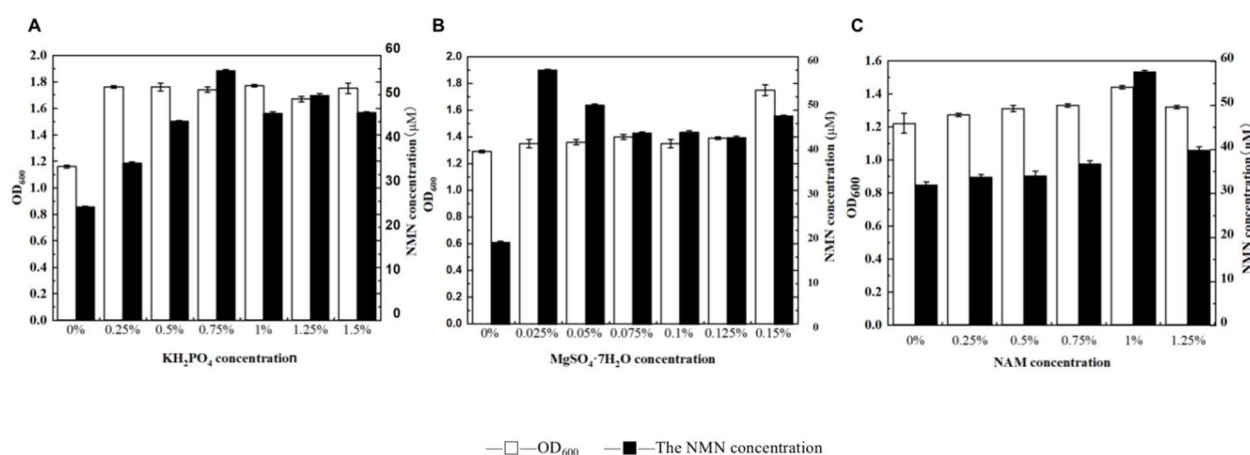
Figure 6. Effects on *Enterobacter chengduensis* 2021T4.7's cell growth and NMN production: **(A)** KH_2PO_4, **(B)** $MgSO_4 \cdot 7H_2O$, and **(C)** NAM.

Among the mineral elements that microorganisms require, magnesium is the active group of some enzymes in cells. Magnesium plays a role in regulating cytoplasmic membrane permeability and controlling the state of cytoplasmic colloids and cellular metabolic activity. We investigated the effect of $MgSO_4 \cdot 7H_2O$ content on the growth of *Enterobacter chengduensis* 2021T4.7 and its ability to produce NMN. As shown in **Figure 6(B)**, the fermentation medium with 0.025% $MgSO_4 \cdot 7H_2O$ was the best in NMN production capacity, and the NMN yield was 57.24 μM.

2.2.4. Effect of NAM inducer on production of NMN by *Enterobacter chengduensis* 2021T4.7

Enzymes in microbial cells can be divided into two categories: induction enzymes and constituent enzymes. The presence of an inducer (usually a reaction substrate) in the environment is required to produce inducible enzymes. The synthesis of inducible enzymes depends on the inducer and gene control in the environment. Constituent enzymes exist in the cell itself and its synthesis is controlled only by the genetic material. **Figure 6(C)** shows that the *Enterobacter chengduensis* 2021T4.7 strain can produce NMN when the medium did not contain NAM. However, with the increase of NAM inducer content in the medium, the yield of NMN also increased, indicating that the ability of *Enterobacter chengduensis* 2021T4.7 to produce NMN can be increased by a NAM-induced culture. When the NAM addition amount was 1%, the strain growth and NMN yield were optimal, with the NMN yield reaching 57.67 μM (**Figure 6(C)**). Therefore, 1% NAM was added to the fermentation medium in subsequent experiments.

2.3. Optimization of fermentation conditions for NMN production by *Enterobacter chengduensis* 2021T4.7

2.3.1. Optimization of initial fermentation pH

Usually, microorganisms can only grow in a specific pH range, and different microorganisms have different pH requirements. Too high or too low of a pH is not conducive to their growth and metabolism. The pH range reflects a microorganism's ability to adapt to the environment, and the optimal pH range for growth pH or enzyme production is often narrow. Therefore, optimizing the initial pH of the fermentation medium is necessary. From **Figure 7(A)**, *Enterobacter chengduensis* 2021T4.7 was very adaptable to the environment and can grow at pH 5.0–9.0. When the initial pH was 7.0, the growth of the bacteria was the best. When the pH was 10.0, the growth of the bacteria stopped. On the other hand, the NMN production capacity first increased and then decreased with pH, and the amplitude was large. NMN production was the most robust at 58.85 μM at an initial pH of 7.0 (**Figure 7(A)**). Thus, the initial pH of the fermentation medium was taken as 7.0 in subsequent experiments.
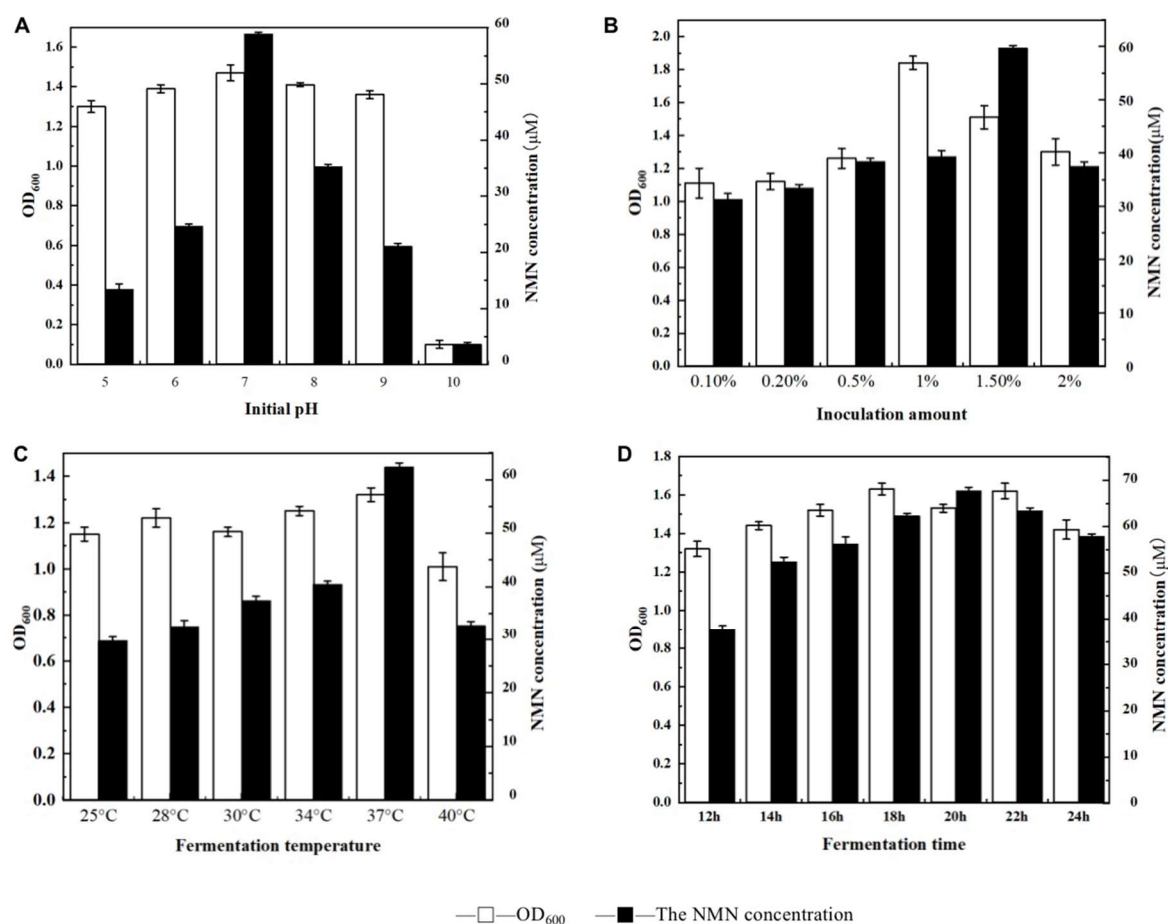
Figure 7. Effect of fermentation conditions on *Enterobacter chengduensis* 2021T4.7's cell growth and NMN production: **(A)** initial pH, **(B)** inoculation amount, **(C)** fermentation temperature, and **(D)** fermentation time.

2.3.2. Optimization of inoculation of fermented cultures

The amount of seeding affects the rate of microbial cell doubling and the length of the growth retardation period. **Figure 7(B)** shows that the growth of the strain was the best when the inoculation amount was 1%, and when the inoculation amount was 1.5%, the strain produced the highest amount of NMN, reaching 59.63

μM. Therefore, the fermentation medium was inoculated at 1.5% inoculation volume in subsequent experiments.

2.3.3. Optimization of fermentation temperature

The effect of fermentation ambient temperature on bacterial growth is manifested in the following aspects: (1) affecting the solubility of substances, (2) affecting the absorption of nutrients and secretion of metabolites by cells, and (3) affecting enzyme activity. **Figure 7(C)** shows that at temperature 25–37 °C, the growth of the strain did not produce significant fluctuations. When the temperature was 40 °C, the growth of the bacteria was inhibited. NMN yield was the highest at 62.36 μM at 37 °C. Therefore, the fermentation medium was inoculated at 37 °C in subsequent experiments.

2.3.4. Optimization of fermentation time

Different fermentation times will also specifically impact bacteria's growth and metabolism. This experiment investigated the effects of different fermentation and culture times on the growth and NMN production capacity of *Enterobacter chengduensis* 2021T4.7. With the increased incubation time, bacterial density and NMN yield first increased and decreased (**Figure 7(D)**). When the incubation time was 18 h, the bacterial density was the largest. When the culture reached 20 h, the ability to produce NMN was the strongest and the maximum yield of NMN was 67.66 μM (**Figure 7(D)**)

3. Clonal expression of mice-derived Nampt (mNampt) and mutants

3.1. Cloning and expression of mNampt

A mice-derived Nampt (mNampt) sequence (**Table 1**) was synthesized by Suzhou Jinweizhi Company after codon optimization. The target gene contained the digestion sites Hind III and Nde I at both ends and a 6×His tag was added at the end. Recombinant vectors containing mNampt target genes (pET-30a(+), pET-24a, pET-28a, ppsumo, psj-2, psj-5) were introduced into host strains *E. coli* BL21(DE3), *E. coli* BL21(DE3)plySs, and Rosetta (DE3). Then, the target protein in multiple vectors and hosts was expressed, and it was found that only *E. coli* BL21 (DE3)-ppsumo-mNampt was successfully expressed. In this expression strain, the mNampt was fused to a SUMO tag. *E. coli* BL21 (DE3)-ppsumo-mNampt protein expression electrophoresis was shown in **Figure 8(A)**. Because a His tag was added to the end of the gene sequence for synthesis, the protein can be purified using magnetic beads, and the buffer of the enzyme after the His-tag purification scheme remained unchanged. The protein electrophoresis diagram of SDS-PAGE after protein purification is shown in **Figure 8(B)**, and the protein bands in the figure were visible, and there were no apparent hetero-proteins in the background.

Table 1. Primers and gene sequences.

Primer	Sequence (5′→3′)	Reference
Nampt-F	TAATCCTTATTCAGTGGTGGTGGTGGTGGTGCTC	This study
Nampt-R	AGGAAGCTTGCATATGAACGCTGCTGCTG	
N67K-F	CGGGCTTCAGTATATTCTTAAAAAATATCTTAAAGG	
N67K-R	TTTAAGAATATACTGAAGCCCGTAGAACACTGT	
S155I-F	GGATTGAAACAATTCTTGTTCAGATCTGGTATCCTA	
S155I-R	GATCTGAACAAGAATTGTTTCAATCCAGTTTG	
N164L-F	CCTATTACAGTTGCTACACTGTCACGCGAAC	
N164L-R	CAGTGTAGCAACTGTAATAGGATACCAT	
R166W-F	GTTGCTACAAACTCATGGGAACAGAAGAAG	
R166W-R	CCATGAGTTTGTAGCAACTGTAATAGGATACC	
A208G-F	GGAAACAGCTGGCATTGGCGGCTCAGCTCATCT	
A208G-R	GCCGCCAATGCCAGCTGTTTCCTGTGATGAAAC	

Table 1. (*Continued*).

Primer	Sequence (5′→3′)	Reference
A245T-F	CCTGGTTATTCAGTTCCTGCTACCGAACATTCAAC	This study
A245T-R	GGTAGCAGGAACTGAATAACCAGGAACTG	
S248A-F	TCCTGCTGCTGAACATGCGACAATTACAG	
S248A-R	ACTATGTTCAGCAGCAGGAACTGAATAAC	
V365L-F	ATTAACACACTTCAGGAAATTCTGGAAGGCATGAAAC	
V365L-R	CAGAATTTCCTGAAGTGTGTTAATATCAACG	
S382M-F	ATTGAGAATGTCTCATTTGGCATGGGCGGCGCTC	
S382M-R	CATGCCAAATGAGACATTCTCAATGGACC	
V467L-F	AGTGTTCAAGAATGGCAAGCTGACGAAGTCCTACTC	
V467L-R	CAGCTTGCCATTCTTGAACACTGTATGAAGAAG	

Mutant of mNampt	Base change
N67K	AAC→AAA
S155I	TCA→ATC
N164L	AAC→CTG
R166W	CGC→TGG
A208G	GCT→GGC
A245T	GCT→ACC
S248A	TCA→GCG
V365L	GTT→CTG
S382M	TCA→ATG
V467L	GTA→CTG

Gene	Sequence (5′→3′)
Optimized *(E. coli)* sequence of mNampt	CATATGAACGCTGCTGCTGAGGCCGAGTTCAATATATTGTTAGCGACCG ACTCGTACAAGGTCACGCATTATAAACAGTATCCTCCTAACACATCAAA GGTCTACTCATATTTCGAGTGCCGCGAGAAGAAGACGGAGAACTCGAA AGTCCGAAAGGTGAAGTATGAAGAAACAGTGTTCTACGGGCTTCAGTA TATTCTTAACAAATATCTTAAAGGCAAAGTTGTTACAAAGGAGAAGAT CCAGGAAGCTAAAGAAGTTTATCGCGAACATTTCCAAGACGATGTCTT CAATGAGCGCGGCTGGAACTATATTCTTGAGAAGTACGACGGCCATCT TCCTATTGAAGTTAAAGCTGTTCCTGAAGGCTCAGTTATTCCTCGCGGC AACGTCCTGTTTACCGTCGAGAATACGGATCCTGAATGTTATTGGCTTA CAAACTGGATTGAAACAATTCTTGTTCAGTCATGGTATCCTATTACAGT TGCTACAAACTCACGCGAACAGAAGAAGATCCTAGCTAAATATCTTCTT GAAACATCAGGCAACCTTGATGGCCTTGAATATAAACTTCATGATTTCG GGTACCGCGGCGTTTCATCACAGGAAACAGCTGGCATTGGCGCTTCAG CTCATCTTGTTAACTTTAAAGGCACAGATACAGTTGCTGGCATTGCTCT TATTAAGAAGTACTACGGCACAAAGGACCCAGTTCCTGGTTATTCAGTT CCTGCTGCTGAACATTCAACAATTACAGCTTGGGGAAAGGATCATGAG AAGGACGCGTTCGAGCACATTGTTACACAGTTCAGTAGTGTTCCTGTTT CAGTTGTTTCAGATTCTTATGATATTTATAACGCTTGTGAGAAGATCTG GGGAGAGGACCTTCGCCATCTTATTGTTTCACGCTCAACAGAAGCTCCT CTTATTATTCGCCCTGATTCAGGCAACCCTCTTGATACAGTTCTTAAAGT TCTTGATATTCTTGGCAAGAAGTTCCCGGTTACCGAGAATTCCAAGGGT TATAAACTTCTTCCTCCTTATCTTCGCGTTATTCAGGGCGATGGCGTTGA TATTAACACACTTCAGGAAATTGTTGAAGGCATGAAACAGAAGAAGTG GTCCATTGAGAATGTCTCATTTGGCTCAGGCGGCGCTCTTCTTCAGAAA CTTACACGCGATCTTCTTAACTGTTCATTTAAATGTTCTTATGTTGTTAC AAACGGCCTTGGCGTTAACGTGTTCAAAGATCCCGTAGCAGACCCTAA CAAACGCTCAAAGAAGGGTC

3.2. Yield of NMN by *E. coli* BL21(DE3)-ppsumo-mNampt strain

We used high-performance liquid chromatography (HPLC) to determine the peak times of NMN and substrates NAM, PRPP, and ATP. It can be seen that the peak times of NMN, PRPP, ATP, and NAM were 3.826 min, 4.757 min, 4.059 min, and 10.804 min, respectively (**Figure 9**). When these four components were mixed and injected, the peaks were well separated from each other, indicating that the HPLC method can be used to determine the yield of NMN after the reaction. The Nampt crude enzyme solution of *E. coli* BL21(DE3)-ppsumo-mNampt strain was prepared. In the enzyme reaction system, the final concentrations of NAM, PRPP, ATP, $MgCl_2$, and $MnCl_2$ were 1 mM each, and the pH was 7.0. The reaction was carried out at

room temperature for 15 min and heated at 95 °C for 1 min to terminate the enzyme reaction. **Figure 10** shows that the NMN standard had a linear relationship in the range of 0–150 μM, and the NMN-producing amount of mNampt from *E. coli* BL21(DE3)-ppsumo-mNampt strain was calculated to be 84.08 μM (28.08 mg/L).
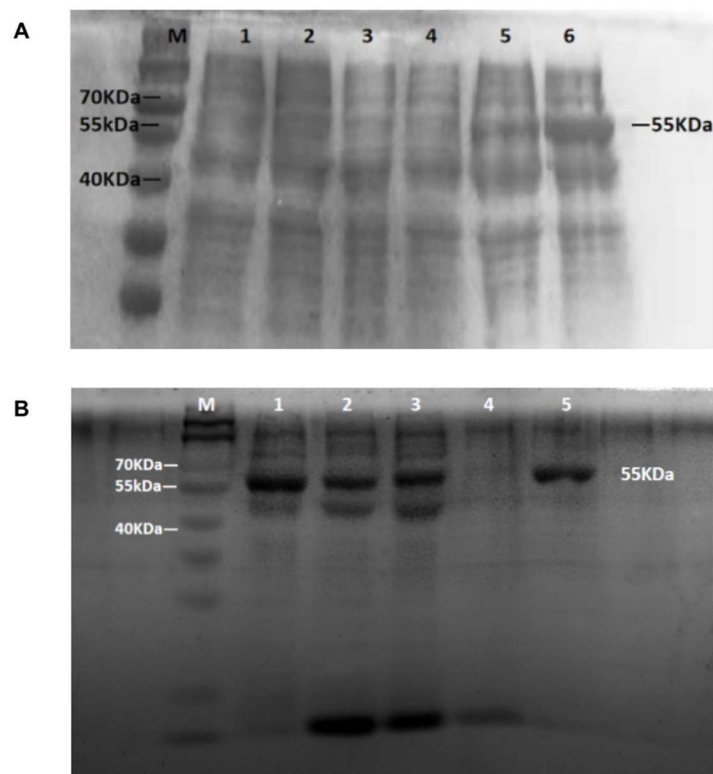
Figure 8. SDS-PAGE electrophoresis diagrams. **(A)** Nampt expression by different hosts/vectors: 1) *E. coli* BL21(DE3)-pET-30a(+)-mNampt(+IPTG 0 h), 2) *E. coli* BL21(DE3)-pET-30a(+)-mNampt(+IPTG 3 h), 3) *E. coli* BL21(DE3)-pET-30a(+)-mNampt(+IPTG 12 h), 4) *E. coli* BL21(DE3)-ppsumo-mNampt(+IPTG 0 h), 5) *E. coli* BL21(DE3)-ppsumo- mNampt(+IPTG 3 h), and 6) *E. coli* BL21(DE3)-ppsumo-mNampt(+IPTG 12 h). **(B)** Nampt purification: M) marker, 1) cell, 2) crude enzyme solution, 3) flow-through solution, 4) eluent, and 5) purified protein.
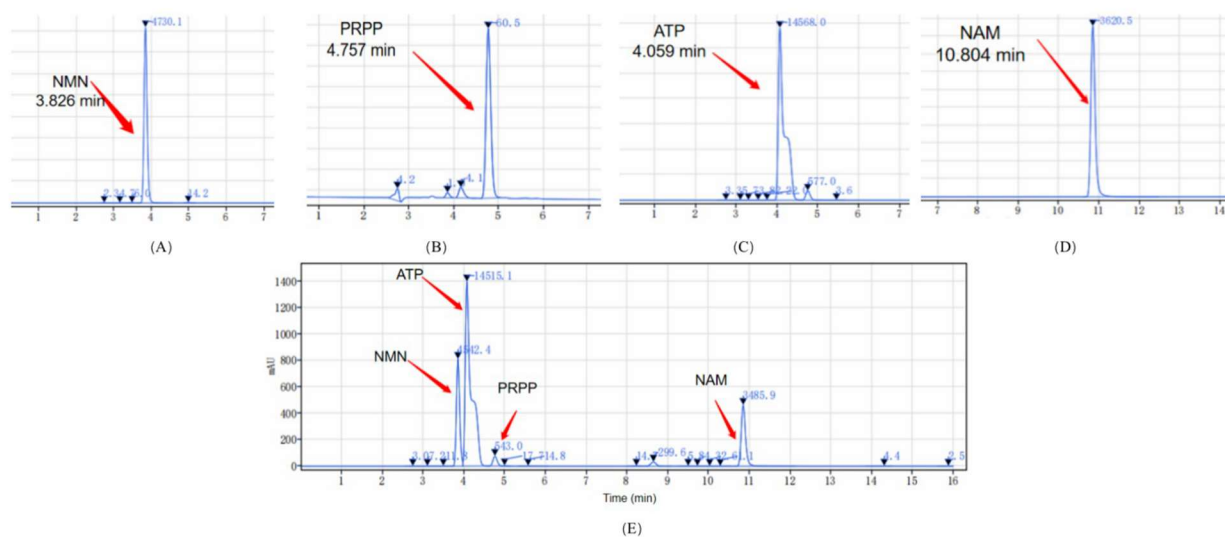
Figure 9. HPLC peaks of **(A)** NMN, **(B)**, PRPP, **(C)** ATP, and **(D)** NAM standards. **(E)** Mixed-sample peak output chart.
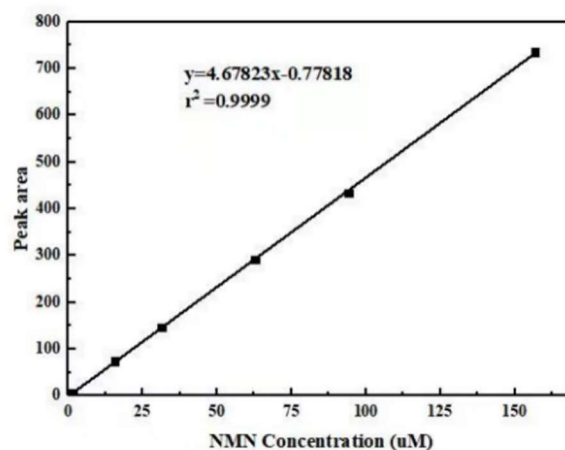
Figure 10. NMN standard curve determined via HPLC.

3.3. Effects of semi-rational design of mNampt on NMN production

Effects of mNampt mutant strains on NMN production

Starting from the enzyme molecule itself, we adopted a semi-rationally designed strategy using a combination of methods based on structural analysis and Gibbs free energy stability. FoldX and DeepDDG software can be used to predict high-quality mutation sites to simulate the effect of mutation sites on Gibbs free energy and protein stability changes. We used FoldX and DeepDDG to simulate and construct the protein structure of mNampt, and then predict its key sites that may affect the catalytic activity of the enzyme. Ten mutation sites were selected from the comprehensive analysis: N67K, S155I, N164L, R166W, A208G, A245T, S248A, V365L, S382M, V467L. Then, site-directed mutant primer PCR amplification primers (**Table 1**) were designed. The primers were synthesized by Guangzhou Aiji Biotechnology. Then, *E. coli* DH5α-ppsumo-mNampt expression strains were constructed. The result of NMN production by the mNampt mutant strain showed that 8 of the 10 cloned mutants had higher mutant activity than those of wild-type strains, among which mNampt-V365L mutant had the highest activity and its yield of NMN was 135.99 μM, or 45.42 mg/L, which was 62% higher than that of wild-type mNampt (84.17 μM, or 28.11 mg/L) (**Figure 11**). The NMN yields of Nampt-S248A, Nampt-N164L, Nampt-S382M, Nampt-A245T, and Nampt-A208G increased by 34%, 27%, 27%, 22%, and 17%, respectively, compared with those of the wild types, while the NMN yields of Nampt-V467L and S155I decreased by 53% and 31%, respectively.
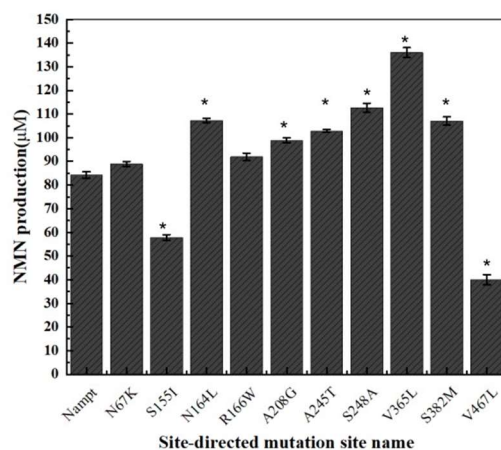
Figure 11. Effect of mNampt site-directed mutagenesis versus wild-type mNampt (control) on NMN production.
Note: *: $p \leq 0.05$.

4. Discussion

With the growing momentum of research on NAD$^+$ biology, many important insights have been provided into aging-related functional decline and disease pathogenesis. Supplementation with these NAD$^+$ intermediates, such as NR and NMN, has shown preventive and therapeutic efficacy, improving aging-related pathophysiology and disease status. There are relatively few research reports on chassis strains that produce NMN. In addition, the technical route of NMN production by Nampt also has problems, such as the low catalytic activity of Nampt and the limited sources of Nampt. Therefore, natural strains with a high yield of NMN were screened from soil in this study and a high-quality and efficient Nampt expression system was constructed to improve the yield of NMN. Bangtai Bioengineering (Shenzhen) Co., Ltd., is an NMN API manufacturer, so collecting soil near the sewer pipeline of its factory was expected to obtain high-NMN-yield strains. Seven strains with a strong ability to transform nicotinamide to generate NMN in soil were selected through preliminary screening and re-screening, among which the highest NMN yield was 44.7 μM and the lowest was 36.59 μM **(Figure 3)**. In addition, strains 3-4 and 4-7 were identified as belonging to the genus Enterobacteriaceae, and to our knowledge, there have been no previous reports of NMN production with Enterobacteriaceae as the microbial chassis. After optimizing the fermentation condition, including the optimization of the fermentation medium, the NMN yield of *Enterobacter chengduensis* 2021T4.7 strain was up to 67.66 μM, or 22.61 mg/L **(Figure 7(D))**. Sugiyama et al. used an NR-nutrient-deficient yeast culture medium as a screening tool to select three strains with NMN production activity from 174 facultative anaerobic lactic acid bacteria (all Fructobacilli), with a maximum NMN-production capacity of 2.1 mg/L[30]. Compared with other strains in previous reports, *Enterobacter chengduensis* 2021T4.7 demonstrated its potential as a natural strain with high-NMN production.

The key to microbial synthesis of NMN is to obtain a strain expressing high Nampt catalytic activity. In this study, a gene sequence of mice-derived Nampt (mNampt) was synthesized and optimized according to *E. coli* codon preference. It was then constructed on a pET-30a(+) vector with *E. coli* BL21 (DE3) as a host cell, which was induced to express it, but the protein failed to express after SDS-PAGE electrophoresis validation. The "Tree of Life" is a phylogenetic tree constructed from the sequenced genomes, and Gazzaniga et al. reported microbial nicotinamide metabolism throughout the Tree of Life[31]. According to the Tree of Life, most microorganisms expressing Nampt may be pathogenic. Therefore, the effects of different vectors and host cells on the expression of mNampt were explored to find the suitable vector and expression host of the enzyme gene. We tested six recombinant vectors (pET-30a(+), pET-24a, pET-28a, ppsumo, psj-2, and psj-5) and three expression hosts (*E. coli* BL21 (DE3), *E. coli* BL21 (DE3) plySs, and Rosetta (DE3)) and found that only *E. coli* BL21 (DE3)-ppsumo-mNampt was successfully expressed. This is different from the combination of *E. coli* BL21(DE3)pLysS and pET-28a(+) vector previously reported by Marinescu et al.[16]. This may be because the Nampt selected by Marinescu et al. was derived from *Haemophilus ducreyi*, which is closer to *E. coli* in the Tree of Life. Although mice-derived Nampt is farther from *E. coli* in the Tree of Life, we obtained an NMN yield of 28.08 mg/L for strain *E. coli* BL21(DE3)-ppsumo-mNampt, which was nearly twice as high as that of the expression strain derived from *Haemophilus ducreyi*. It is difficult to obtain a highly efficient soluble expression of Nampt in *E. coli*. At first, we used a pET expression system, but the target protein expression was very low. In recent years, SUMO has been found to be a molecular chaperone to increase the stability and solubility of foreign proteins. Its mechanism may be that SUMO protein, as a highly hydrophobic core, provides nucleation sites for the folding of target proteins[32], promotes the interaction between proteins to enable them to fold correctly, and finally enhances the solubility of fusion proteins[33].

If the structural information and mechanism of enzyme molecules are understood, semi-rational design or rational design methods are the preferred methods for customizing efficient biocatalysts[28,34], and many

articles have reported the use of semi-rational design methods to improve the catalytic activity, stability, substrate specificity, etc., of enzymes[27–29]. We used FoldX and DeepDDG software to analyze the structure of the target protein Nampt, predicted 10 sites that may affect enzyme activity, and carried out a semi-rational design of enzymes. We obtained 10 mutants, 8 of which were more active than the wild types (**Figure 12**). Among them, Nampt-V365L mutant had the highest activity, where the conversion rate was 13.60% and the yield of NMN was 135.99 μM (45.42 mg/L), which was 62% higher than that of the wild type (28.11 mg/L). The mutation from neutral non-polar valine to neutral non-polar leucine at the Nampt-V365 site indicated that leucine positively affected enzyme activity. Secondly, the catalytic activity of mutant Nampt-S248A was 34% higher than that of the wild-type strain, indicating that hydrophobic amino acids are beneficial to improve the environment in this region to increase the stability of Nampt. The result also showed that some mutants may reduce the side effect of enzyme activity. For example, Nampt-V467L mutated from valine to acid leucine and significantly reduced enzyme activity, and the NMN yield of this strain was only 39.97 μM, which decreased by 53% compared with the wild type (**Figure 12**). In addition, the NMN yield of Nampt-S155I also decreased by 31% compared with that of the wild type. This indicates that Nampt V467 and S155 are crucial for the enzyme activity of Nampt.
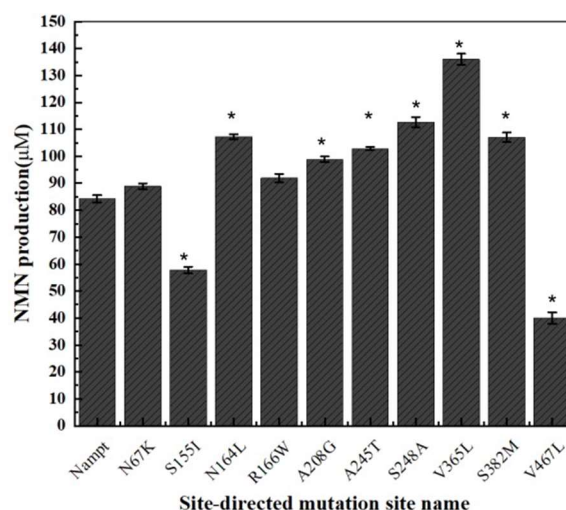
Figure 12. Effect of mNampt site-directed mutagenesis versus wild-type mNampt (control) on NMN production.
Note: *: $p \leq 0.05$.

It has been shown that site 365 of mNampt may be a key site affecting enzyme activity. From the structural point of view, valine is longer and more hydrophobic than the leucine aliphatic side chain, which makes the nearby protein structure more stable, suggesting that the stabilization of the protein structure in the V365 region can enhance the affinity of mNampt enzyme protein for the NAM substrate. Mutant V365L catalyzed 135.99 μmol/L (45.42 mg/L) of NMN under the same condition, which was 62% higher than that of wild-type mNampt (**Figure 12**) and 2.6-fold higher than the yield of the recombinant *E. coli* MNM expression strain (17.26 mg/L) constructed by Marinescu et al.[16]. Liao et al. overexpressed Nampt from *Meiothermus ruber* in *E. coli* and used PRPP and NAM as substrates for enzymatic reaction for 10 min to obtain 34 mg/L of NMN[35]. To our knowledge, the NMN content of 45.42 mg/L is the best production in *E. coli*. From existing evidence, an increase in the hydrophobic area can help improve the stability of the structure near site 365 of mNampt. We speculate that the stabilization of the structure in this region increases the affinity of the enzyme protein for the NAM substrate, resulting in a tighter binding pocket formed during the enzyme catalysis process, which constitutes an effective steric hindrance[36].

In mammals, the salvage pathway starting from NAM is the main NAD^+ biosynthetic pathway[37]. The biosynthetic production of NMN is generally based on NAM and PRPP as substrates, and NMN is generated under the catalysis of Nampt (**Figure 1**). The phosphate in NMN is mainly derived from energy substances, such as ATP or PRPP (**Figure 1**). The market price of these two precursors is high, which also leads to the high production cost of this method, seriously restricting its application and development. In the future, the biosynthetic pathway can be improved through synthetic biology methods, bypassing the pathway of PRPP and ATP as energy substances by using cheap NAM and NR as starting materials, which can significantly reduce production costs and promote the promotion of NMN industrial production. The one-step conversion of NR to NMN has been considered to be the most promising synthetic route for NMN. He et al.[38] used whole-cell NRK-2 as the catalyst under optimized conditions, and the NMN yield was up to 12.6 g/L in the reaction mixture, which was much higher than those in previous reports. Huang et al.[39] fermented and synthesized NMN using glucose and NAM as substrates. By optimizing the batch feeding process and heterologously expressing Nampt derived from *Vibrio bacteriophage* KVP40 in a 5L bioreactor, the yield of NMN reached 16.2 g/L. This is currently the highest yield of NMN via the fermentation method. In addition, ATP can be directly provided for NMN synthesis through yeast-coupled fermentation, reducing the cost of ATP. NMN extraction and purification technology needs further research and development to reduce its extraction cost.

5. Materials and methods

5.1. Bacterial strains and culture medium

E. coli DH5α purchased from Takara (Japan) was used for plasmid cloning and long-term storage. *E. coli* BL21(DE3), Rosetta (DE3), and *E. coli* BL21(DE3)plySs purchased from Takara were used for protein expression.

Because Nampt uses nicotinamide to generate NMN, a screening medium was designed with nicotinamide as a single carbon source to culture and screen NMN-producing strains. The culture medium used in this study and its composition were as follows. The enrichment medium (pH = 7) was composed of niacinamide (2 g/L), glucose (5 g/L), yeast paste (5 g/L), peptone (5 g/L), $K_2HPO_4 \cdot 3H_2O$ (14 g/L), KH_2PO_4 (5.2 g/L), and $MgSO_4 \cdot 7 H_2O$ (2 g/L). The screening medium (pH = 7) was composed of an enriched medium formulation to remove glucose, as well as $MgSO_4 \cdot 7H_2O$ (14 g/L). The plate isolation medium was agar powder (12.5 g/L) added to the screening medium. The culture preservation medium (pH = 7) was composed of tryptone (10 g/L), yeast extract (5 g/L), and NaCl (5 g/L). The seed medium (pH = 7) was composed of tryptone (10 g/L), yeast extract (5 g/L), $(NH_4)_2SO_4$ (1 g/L), $K_2HPO_4 \cdot 3H_2O$ (2.5 g/L), and $MgSO_4 \cdot 7H_2O$ (0.5 g/L). The fermentation medium (pH = 7) was composed of nicotinamide (1 g/L), tryptone (10 g/L), $(NH_4)_2SO_4$ (1 g/L), K_2HPO_4 (2.5 g/L), and $MgSO_4 \cdot 7H_2O$ (0.5 g/L).

5.2. Natural high-NMN-yield strain screening

A soil sample was collected near the drainage pipe at Bangtai Biotechnology. Excess components were removed and a seed solution (10 mL/50 mL) was prepared after pre-treatment. The solution was shaken in a constant-temperature shaker (180 rpm) at 37 °C for 15 min. The seed solution was added to a fermentation medium (10 mL/50 mL) with 1% inoculation and incubated under the same condition for 12h. A 1mL bacterial solution was prepared into a crude enzyme solution and enzyme reaction system (50 mM Tris HCl buffer, 0.02% bovine serum protein BSA, 12 mM $MgCl_2$, 2 mM ATP, 2 mM dithiothreitol, 80 μM nicotinamide, 40 μM 5-phosphate ribose-1-pyrophosphate (PRPP), and 12.5 μL bacterial solution). Among them, PRPP was unstable and needed to be freshly prepared. After reacting at 95 °C for 1 min, the reaction was terminated by cooling on ice. The NMN content at OD_{445} was detected using an enzyme-linked immunosorbent assay (Tecan, BioTek,

USA) and the conversion rate was calculated. The selected strains were stained using the Gram staining method and sent to Guangzhou Aiji Biotechnology for 16S rDNA sequencing identification.

5.3. Construction of protein expression vectors

Protein expression vectors pET-30a(+), pET-28a(+) and pET-24a(+) were preserved in our laboratory. Protein expression vectors ppsumo, psj-2, and psj-5 were donated by EZ-lab of the Institute of Advanced Technology, Chinese Academy of Sciences. These vectors were all *E. coli* protein expression vectors, with the PET vector having an N-terminal T7 tag and a C-terminal His tag, while the ppsumo vector contained a SUMO tag. The recombinant nicotinamide phosphoribosyltransferase gene sequence derived from mice (mNampt) (**Table 1**) was synthesized by Suzhou Jinweizhi Co., Ltd. The mNampt gene sequence was optimized for expression in *E. coli* (considering the frequency of codon usage and GC content and eliminating unwanted restriction sequences), containing digestion sites Hind III and Nde I at both ends and a 6×His tag added at the end of the sequence.

The mNampt gene was digested by Hind III and Nde I double enzymes and cloned in the pET-30a(+) expression vector, which permitted protein expression under the control of the T7*lac* promoter. The mNampt gene was also cloned to pET-28a(+), pET-24a(+), ppsumo, psj-2, and psj-5 using the same method. Six plasmids were produced, which were mNampt-PET vectors containing the Nampt gene from mice, cloned in *E. coli* DH5α, and maintained (as a glycerol stock) at −80 ℃. The resulted plasmids were chemically transformed into the competent *E. coli* DH5α. The transformed kanamycin-resistant bacteria were selected on agar plates. The vectors' presence was verified via 1% agarose gel electrophoresis and PCR amplification with Nampt-F forward and Nampt-R primers (**Table 1**). Cloning and transformation were performed into the different expression strains (*E. coli* BL21(DE3), Rosetta (DE3), and *E. coli* BL21(DE3)plySs) in order to express the Nampt enzymes.

The semi-rational design of mNampt mutant plasmid used ppsumo-Nampt(m) plasmid as the template. FoldX and DeepDDG software were used to predict the high-quality mutation sites of mNampt. The point-mutant PCR amplification primers (**Table 1**) were synthesized by Guangzhou Aiji Biotechnology, and the mutation sequence was obtained by amplification separately. Then the recombinant ppsumo-mNampt mutant plasmid was constructed according to the manual method of the homologous recombinant kit (Novazan Biotechnology). The vectors' presence was verified via 1% agarose gel electrophoresis and PCR amplification with Nampt-F forward and Nampt-R primers (**Table 1**). Cloning and transformation were performed into *E. coli* BL21(DE3).

5.4. Bacterial growth condition

For plasmid cloning, initial evaluation of recombinant protein expression, determination of tolerated NAM concentration in a growth medium, and optimization of protein induction and cell density, the bacteria were grown in a shake-flask (180 rpm) incubator at 37 ℃ in an LB medium supplemented with antibiotics for plasmid maintenance (50 μg/mL kanamycin for expression vectors and 25 μg/mL chloramphenicol for pLysS plasmid). Bacterial growth kinetics were recorded as cell density, measured as 600 nm light scattering using a spectrophotometer.

For the inducible expression strain of mNampt, the bacterial strain was inoculated into a seed medium, incubated at 180 rpm, shaken for 12 h at 37 ℃, and then transferred to a kanamycin-containing fermentation medium at 1% inoculation. Then, the fermentation medium of kanamycin was expanded under the same condition at 2% inoculation, and when the optical density (OD) was between 0.5–0.6, 0.25 mM IPTG was added and expression was induced for 16 h at 18 ℃. The protein presence was confirmed via SDS-PAGE (8% resolving gel and 4% stacking gel).

5.5. Transformation of bacteria

Approximately 100 μL of chemically competent cells were mixed with 1 μL plasmidial DNA resulting either from the miniprep (0.2 μg/μL plasmids carrying synthesized mNampt). The tubes were placed for 30 min on ice, followed by heat shock for 45 s in a water bath preheated at 42 °C, and then cooled on ice for 2 min. Then, 700 μL of the LB medium was added and the bacteria were incubated for 1 hour at 37 °C under shaking at 180 rpm. The cells were inoculated on agar Petri dishes with specific antibiotics for selection (10 μL/plate) and left overnight at 37 °C. The next day, single colonies were selected from each plate and inoculated in the LB medium containing the antibiotics for plasmid maintenance. After one day, plasmid DNA was extracted from 1 mL of the overnight culture using a plasmid extraction kit from Omega Bio-Tek. The presence of the cloned vectors was confirmed via 1% agarose gel electrophoresis. DNA concentration and purity were determined using a NanoDrop spectrophotometer (Thermo Scientific).

Production of NMN through Nampt crude enzyme solution

The induced bacterial solution was adjusted to OD_{600} to 1.0 using a PBS buffer with pH 7.4 and then concentrated five-fold to produce a crude Nampt enzyme solution. A crude enzyme solution of 12.5 μL and mother liquor of 12.5 μL (1 mM niacinamide, 1 mM ATP, 1 mM PRPP, 1 mM $MgCl_2$, and 1 mM $MnCl_2$) were added evenly and reacted at room temperature for 15 min. The reaction solution was heated in a 95 °C metal bath for 1 min to inactivate the enzyme.

5.6. Protein purification

Bacterial cells were separated from the growth media by centrifugation at 3000× g. The supernatant was collected separately and the cells were re-suspended in the same volume of water and lysed via sonication using a Soniprep 150 Ultrasonic Crusher (Sanyo) on ice for 10 min (5 s with a 5-s pause). The crumbled crude enzyme solution was stored at –20 °C. Protein was purified using the His•Bind purification kit (Novagen, Merck KGaA, Darmstadt, Germany) and desalted according to the manufacturer's protocols. The protein concentration was determined via a BSA protein quantitation kit (Amresco) using bovine serum albumin as the standard.

5.7. Fluorometric NMN Assay

The fluorometric derivatization method was adapted for the 96-well plates with 50 μL of reaction solution, 10 μL of 20% acetophenone, and 20 μL of 2M KOH solution to the black enzyme plate and placed in ice water. After 10 min of incubation on ice, a volume of 90μL 88% formic acid was added to each well and the plate was incubated at 37 °C for 10 min. The UV emission was measured at 445 nm on the spectrophotometer at excitation wavelength of 382 nm. A calibration curve in the concentration range of 0–150 μM with a coefficient of correlation of 0.99 was obtained by interpolating five standard sample dilutions of an external standard NMN. The lysate of bacterial cells from uninduced culture was used as the control.

HPLC method to detect NMN

The detection of NMN via the HPLC method has the characteristics of strong sensitivity and high precision. This method is based on the research by Kurnasov et al.[40] A concentration of 0.1mol/L 100% sodium dihydrogen phosphate solution was selected to separate ATP, NMN, and NR. Methanol was selected as the organic phase and sodium dihydrogen phosphate was used as the mobile phase gradient elute, thereby eluting the debris in the reaction system. After the reaction, protein was removed via microultrafiltration using Microcon YM-10 centrifugal filters (Amicon, Bedford, MA, USA). and the filtrates were analyzed using a ChromCore C18 reversed-phase column (5 μm, 4.6 × 250 mm) after appropriate dilution. Ion pair separation

was carried out isocratically in 0.1mol/L $NaH_2PO_4 \cdot 2H_2O$ (pH 5.5) and a mobile phase (100% methanol methanol) at 1 mL/min. The sample injection volume was 20 μL and the process was monitored at 254 nm with an HPLC system (Gibson, Middleton, WI, USA). The Origin 2019b software was used to process the data and plot a standard curve with NMN concentration as the abscissa and sample peak area as the ordinate.

5.8. Statistical methods

Variance analysis was performed using SPSS v.18 software. Each data point was plotted as mean value ± standard deviation of at least three independent experiments. Statistical significance was defined as $p \leq 0.05$.

Acknowledgments

Conflict of interest

The authors of the article have no conflicts of interest to declare.

References

1. Wang X, Hu X, Yang Y, et al. Nicotinamide mononucleotide protects against β-amyloid oligomer-induced cognitive impairment and neuronal death. *Brain Research* 2016; 1643: 1–9. doi: 10.1016/j.brainres.2016.04.060
2. Khan JA, Forouhar F, Tao X, et al. Nicotinamide adenine dinucleotide metabolism as an attractive target for drug discovery. *Expert Opinion on Therapeutic Targets* 2007; 11(5): 695–705. doi: 10.1517/14728222.11.5.695
3. Fletcher RS, Ratajczak J, Doig CL, et al. Nicotinamide riboside kinases display redundancy in mediating nicotinamide mononucleotide and nicotinamide riboside metabolism in skeletal muscle cells. *Molecular Metabolism* 2017; 6(8): 819–832. doi: 10.1016/j.molmet.2017.05.011
4. Frederick DW, Loro E, Liu L, et al. Loss of NAD homeostasis leads to progressive and reversible degeneration of skeletal muscle. *Cell Metabolism* 2016; 24(2): 269–282. doi: 10.1016/j.cmet.2016.07.005
5. Guan Y, Wang SR, Huang XZ, et al. Nicotinamide mononucleotide, an NAD^+ precursor, rescues age-associated susceptibility to AKI in a sirtuin 1-dependent manner. *Journal of the American Society of Nephrology* 2017; 28(8): 2337–2352. doi: 10.1681/asn.2016040385
6. Uddin GM, Youngson NA, Sinclair DA, et al. Head to head comparison of short-term treatment with the NAD^+ precursor nicotinamide mononucleotide (NMN) and 6 weeks of exercise in obese female mice. *Frontiers in Pharmacology* 2016; 7. doi: 10.3389/fphar.2016.00258
7. Fukamizu Y, Uchida Y, Shigekawa A, et al. Safety evaluation of β-nicotinamide mononucleotide oral administration in healthy adult men and women. *Scientific Reports* 2022; 12(1). doi: 10.1038/s41598-022-18272-y
8. Nadeeshani H, Li J, Ying T, et al. Nicotinamide mononucleotide (NMN) as an anti-aging health product—Promises and safety concerns. *Journal of Advanced Research* 2022; 37: 267–278. doi: 10.1016/j.jare.2021.08.003
9. Park JH, Long A, Owens K, et al. Nicotinamide mononucleotide inhibits post-ischemic NAD^+ degradation and dramatically ameliorates brain damage following global cerebral ischemia. *Neurobiology of Disease* 2016; 95: 102–110. doi: 10.1016/j.nbd.2016.07.018
10. Yano M, Akazawa H, Yabumoto C, et al. Monocyte–derived extracellular Nampt-dependent biosynthesis of NAD^+ protects the heart against pressure overload. *Journal of Cardiac Failure* 2015; 21(10): S178. doi: 10.1016/j.cardfail.2015.08.188
11. Mills KF, Yoshida S, Stein LR, et al. Long-term administration of nicotinamide mononucleotide mitigates age-associated physiological decline in mice. *Cell Metabolism* 2016; 24(6): 795–806. doi: 10.1016/j.cmet.2016.09.013

12. Long AN, Owens K, Schlappal AE, et al. Effect of nicotinamide mononucleotide on brain mitochondrial respiratory deficits in an Alzheimer's disease-relevant murine model. *BMC Neurology* 2015; 15(1). doi: 10.1186/s12883-015-0272-x

13. Revollo JR, Körner A, Mills KF, et al. Nampt/PBEF/visfatin regulates insulin secretion in β cells as a systemic NAD biosynthetic enzyme. *Cell Metabolism* 2007; 6(5): 363–375. doi: 10.1016/j.cmet.2007.09.003

14. Caton PW, Kieswich J, Yaqoob MM, et al. Nicotinamide mononucleotide protects against pro-inflammatory cytokine-mediated impairment of mouse islet function. *Diabetologia* 2011; 54(12): 3083–3092. doi: 10.1007/s00125-011-2288-0

15. Stromsdorfer KL, Yamaguchi S, Yoon MJ, et al. NAMPT–mediated NAD$^+$ biosynthesis in adipocytes regulates adipose tissue function and multi-organ insulin sensitivity in mice. *Cell Reports* 2016; 16(7): 1851–1860. doi: 10.1016/j.celrep.2016.07.027

16. Marinescu GC, Popescu RG, Stoian G, et al. β-nicotinamide mononucleotide (NMN) production in *Escherichia coli*. *Scientific Reports* 2018; 8(1). doi: 10.1038/s41598-018-30792-0

17. Marinescu GC, Popescu RG, Dinischiotu A. Size exclusion chromatography method for purification of nicotinamide mononucleotide (NMN) from bacterial cells. *Scientific Reports* 2018; 8(1). doi: 10.1038/s41598-018-22806-8

18. Wang P, Xu TY, Guan YF, et al. Perivascular adipose tissue–derived visfatin is a vascular smooth muscle cell growth factor: Role of nicotinamide mononucleotide. *Cardiovascular Research* 2008; 81(2): 370–380. doi: 10.1093/cvr/cvn288

19. van der Veer E, Ho C, O'Neil C, et al. Extension of human cell lifespan by nicotinamide phosphoribosyltransferase. *Journal of Biological Chemistry* 2007; 282(15): 10841–10845. doi: 10.1074/jbc.c700018200

20. Burgos ES, Schramm VL. Weak coupling of ATP hydrolysis to the chemical equilibrium of human nicotinamide phosphoribosyltransferase. *Biochemistry* 2008; 47(42): 11086–11096. doi: 10.1021/bi801198m

21. Cobb RE, Chao R, Zhao H. Directed evolution: Past, present, and future. *AIChE Journal* 2013; 59(5): 1432–1440. doi: 10.1002/aic.13995

22. Bommarius AS. Biocatalysis: A status report. *Annual Review of Chemical and Biomolecular Engineering* 2015; 6(1): 319–345. doi: 10.1146/annurev-chembioeng-061114-123415

23. Reetz MT. Biocatalysis in organic chemistry and biotechnology: Past, present, and future. *Journal of the American Chemical Society* 2013; 135(34): 12480–12496. doi: 10.1021/ja405051f

24. Chen Z, Zeng A. Protein design in systems metabolic engineering for industrial strain development. *Biotechnology Journal* 2013; 8(5): 523–533. doi: 10.1002/biot.201200238

25. Kipnis Y, Dellus-Gur E, Tawfik DS. TRINS: a method for gene modification by randomized tandem repeat insertions. *Protein Engineering Design and Selection* 2012; 25(9): 437–444. doi: 10.1093/protein/gzs023

26. Cheng F, Zhu L, Schwaneberg U. Directed evolution 2.0: improving and deciphering enzyme properties. *Chemical Communications* 2015; 51(48): 9760–9772. doi: 10.1039/c5cc01594d

27. Yu H, Qiu S, Cheng F, et al. Improving the catalytic efficiency of aldo-keto reductase KmAKR towards t-butyl 6-cyano-(3R,5R)-dihydroxyhexanoate via semi-rational design. *Bioorganic Chemistry* 2019; 90: 103018. doi: 10.1016/j.bioorg.2019.103018

28. Zhang Q, Lu X, Zhang Y, et al. Development of a robust nitrilase by fragment swapping and semi-rational design for efficient biosynthesis of pregabalin precursor. *Biotechnology and Bioengineering* 2019; 117(2): 318–329. doi: 10.1002/bit.27203

29. Xu P, Ni ZF, Zong MH, et al. Improving the thermostability and activity of Paenibacillus pasadenensis chitinase through semi-rational design. *International Journal of Biological Macromolecules* 2020; 150: 9–15. doi: 10.1016/j.ijbiomac.2020.02.033

30. Sugiyama K, Iijima K, Yoshino M, et al. Nicotinamide mononucleotide production by fructophilic lactic acid bacteria. *Scientific Reports* 2021; 11(1). doi: 10.1038/s41598-021-87361-1

31. Gazzaniga F, Stebbins R, Chang SZ, et al. Microbial NAD metabolism: Lessons from comparative genomics. *Microbiology and Molecular Biology Reviews* 2009; 73(3): 529–541. doi: 10.1128/mmbr.00042-08

32. Malakhov MP, Mattern MR, Malakhova OA, et al. SUMO fusions and SUMO-specific protease for efficient

expression and purification of proteins. *Journal of Structural and Functional Genomics* 2004; 5(1–2): 75–86. doi: 10.1023/B:JSFG.0000029237.70316.52

33. Johnson ES. Protein modification by SUMO. *Annual Review of Biochemistry* 2004; 73(1): 355–382. doi: 10.1146/annurev.biochem.73.011303.074118

34. Lutz S. Beyond directed evolution–semi-rational protein engineering and design. *Current Opinion in Biotechnology* 2010; 21(6): 734–743. doi: 10.1016/j.copbio.2010.08.011

35. Liao YB, Wu MH, Ling SL, et al. Expression of nicotinamide phosphoribosyltransferase in *Escherichia coli* and catalytic synthesis of nicotinamide mononucleotide. *Modern Food Science and Technology* 2021; 37(2): 87–93, 182.

36. Reetz MT, Carballeira JD. Iterative saturation mutagenesis (ISM) for rapid directed evolution of functional enzymes. *Nature Protocols* 2007; 2(4): 891–903. doi: 10.1038/nprot.2007.72

37. Imai S, Yoshino J. The importance of Nampt/NAD/SIRT1 in the systemic regulation of metabolism and ageing. *Diabetes, Obesity and Metabolism* 2013; 15(s3): 26–33. doi: 10.1111/dom.12171

38. He Z, Yang X, Tian X, et al. Yeast cell surface engineering of a nicotinamide riboside kinase for the production of β–nicotinamide mononucleotide via whole–Cell catalysis. *ACS Synthetic Biology* 2022; 11(10): 3451–3459. doi: 10.1021/acssynbio.2c00350

39. Huang Z, Li N, Yu S, et al. Systematic engineering of *Escherichia coli* for efficient production of nicotinamide mononucleotide from nicotinamide. *ACS Synthetic Biology* 2022; 11(9): 2979–2988. doi: 10.1021/acssynbio.2c00100

40. Kurnasov OV, Polanuyer BM, Ananta S, et al. Ribosylnicotinamide kinase domain of NadR protein: Identification and implications in NAD^+ biosynthesis. *Journal of Bacteriology* 2002; 184(24): 6906–6917. doi: 10.1128/jb.184.24.6906-6917.2002